

Acoustic interaction force between two particles immersed in a viscoelastic fluid

Fatemeh Eslami,¹ Hossein Hamzehpour,^{1, a)} Sanaz Derikvandi,¹ and S. Amir Bahrani^{2, b)}

¹⁾*Department of Physics, K.N. Toosi University of Technology, Tehran 15875-4416, Iran.*

²⁾*IMT Nord Europe, Institut Mines Télécom, Univ. Lille, Center for Energy and Environment, F-59000 Lille, France.*

(Dated: 18 January 2023)

The interaction acoustic radiation force in a standing plane wave applied to each small solid sphere in a two-particle system immersed in a viscoelastic fluid is studied in a framework based on perturbation theory. In this work, the first- and second-order perturbation theories are used in the governing equations with considering the upper-convected maxwell model to obtain mathematical modeling. We use the finite element method to carry out simulations and describe the behavior of the viscoelastic fluid. The mathematical development is validated from three literature case studies: a one-particle system in a viscous fluid, a two-particle system in a viscous fluid, and a one-particle system in a viscoelastic fluid. The novelty of this study is to establish the acoustic interaction force between two spherical particles immersed in a viscoelastic fluid. The results show that the acoustic interaction force between two spheres is greater in a viscous fluid in comparison with the viscoelastic fluid with the same shear viscosity. This behavior is due to the relaxation time effect. A mathematical formula is proposed for the acoustic interaction force between particles located close to each other in a viscoelastic fluid.

Introduction. Many studies have been done on particle manipulation using acoustophoresis which is essential for analyzing micro-sized particles in numerous biological and chemical applications¹⁻⁴. Acoustophoresis is the movement of particles in micro-channels by ultrasound. Particles exposed to an external acoustic wave that is mainly a standing wave, are subjected to a time-averaged force from scattering waves called the acoustic radiation force⁵⁻¹². For a two-particle system in an acoustic field, the total radiation force applied to each particle consists of primary and secondary forces. The acoustic primary force is due to the incident and the scattered waves from the surface of the particle. The primary force pushes particles into the pressure node or antinode depending on their acoustic contrast factor¹². The secondary (interaction) force is exerted on each particle owing to the effect of the scattered wave from the other one¹³⁻²⁰. In practice, there are many micro-sized particles in biological solutions and suspensions; therefore, the interaction force between them plays a significant role and makes our study important.

At first, the acoustic interaction force was studied by Bjerknæs² to investigate the acoustic inter-particle force between a pair of bubbles, based on the theory of rescattering of scattered waves. Then, Apfel and Embleton³ obtained an approximation for the acoustic interaction force between two spheres using King's and Yosioka's methods^{1,6}. Doinikov and Zavtrak^{21,22} applied the multiple re-expansion method. They used monopole and dipole terms of the multipole series expansion to calculate the primary and interaction forces. Doinikov¹⁰ used five

terms of this expansion to estimate the secondary force between two bubbles in the water. Bruus and Silva²³ in 2014 indicated that the interaction force can be derived from the potential field just like the primary force. Sepehrihahnama and his colleagues¹⁹ in 2016 represented the effect of viscosity and acoustic streaming on the inter-particle radiation force between two rigid spheres and they proposed a numerical algorithm for calculation of the primary and total radiation forces. Their method had no restriction on the size of the spheres because of the use of higher-order multipole terms.

Although particle movement in Newtonian fluids has been widely studied so far^{10,18}, there is little research on particle movement in non-Newtonian fluids. Non-Newtonian fluids such as blood, suspensions, and many other fluids are very ubiquitous in our daily life. Dual et al.²⁴ in 2021 studied the acoustic radiation force on a solid particle in an acoustically excited viscoelastic fluid. They described the fluid motion by the compressible Oldroyd-B model and no restrictions were imposed on the particle size with respect to the acoustic wavelength and the viscous penetration depth in their method.

Another second-order nonlinear effect that is exerted by the incident acoustic wave on the particles is called acoustic streaming²⁵, but in this contribution, our focus is on the acoustic radiation force effect. To our knowledge, there is no study on acoustic interaction force between spheres suspended in a viscoelastic fluid. Therefore it is important to invest our research focus on calculating the acoustic interaction force in non-Newtonian fluids to develop our understanding of particles' behavior inside such fluids.

The novelty of this study is to develop a mathematical model for the acoustic interaction force between two particles immersed in a viscoelastic fluid. The rest of the

^{a)} Electronic mail: hamzehpour@kntu.ac.ir

^{b)} Electronic mail: amir.bahrani@imt-nord-europe.fr

manuscript is organized as follows. First, the theoretical background is expanded by implementing a viscoelastic fluid model in the governing equations of acoustophoresis in the framework of first and second-order perturbation theory^{26–30}. Then, the numerical model and boundary conditions are described. After that, the validation of this contribution is represented. Finally, the results are presented and discussed. The last section concludes the letter.

Theoretical background. In the absence of body forces, the fluid flow governing equations in the microfluidic systems for a viscous fluid are the kinematic continuity equation of ρ and the dynamic Navier-Stokes equation for the velocity field \mathbf{v} , as

$$\partial_t \rho = \nabla \cdot [-\rho \mathbf{v}], \quad (1a)$$

$$\partial_t(\rho \mathbf{v}) = \nabla \cdot [-p \mathbf{I} + \boldsymbol{\tau}]. \quad (1b)$$

The shear stress, $\boldsymbol{\tau}$, of viscous fluid is defined as,

$$\boldsymbol{\tau} = \eta[\nabla \mathbf{v} + (\nabla \mathbf{v})^T] + [\eta_b - \frac{2}{3}\eta](\nabla \cdot \mathbf{v})\mathbf{I}, \quad (2)$$

where η and η_b are the dynamic and bulk viscosities, respectively. For viscoelastic fluids, a variety of models has been reported in the literature^{26,27,31}, to describe such fluids behavior. Here, we consider the Maxwell model³¹ to investigate the effect of viscoelastic fluid on the acoustophoretic forces. In this model, the constitutive equation of fluid is expressed by

$$\boldsymbol{\tau} + \frac{\eta}{G} \frac{\partial \boldsymbol{\tau}}{\partial t} = \eta \dot{\boldsymbol{\gamma}}, \quad (3)$$

where $\dot{\boldsymbol{\gamma}}$ and G are the shear rate and dynamic modulus, respectively. The dot denotes the time derivative. The symmetric $\dot{\boldsymbol{\gamma}}$ is defined as,

$$\dot{\boldsymbol{\gamma}} = [\nabla \mathbf{v} + (\nabla \mathbf{v})^T]. \quad (4)$$

Due to the frame invariance of the stress tensor, the time derivative of $\boldsymbol{\tau}$, is replaced with the upper-convected time derivate as^{31–33}

$$\overline{\nabla} \boldsymbol{\tau} = \frac{\partial \boldsymbol{\tau}}{\partial t} + \mathbf{v} \cdot \nabla \boldsymbol{\tau} - (\nabla \mathbf{v}) \cdot \boldsymbol{\tau} - \boldsymbol{\tau} \cdot (\nabla \mathbf{v})^T. \quad (5)$$

Therefore, the Maxwell model is replaced with the upper-convected Maxwell model (UCM)³¹. In this way, the constitutive equation is represented by

$$\boldsymbol{\tau} + \lambda \overline{\nabla} \boldsymbol{\tau} = \eta \dot{\boldsymbol{\gamma}}, \quad (6)$$

where $\lambda = \eta/G$ is the relaxation time. In this contribution, the governing equations are solved using the perturbation theory^{33–35}.

First-order perturbation. According to the perturbation theory, acoustic variables are considered as,

$$\rho(\mathbf{r}, t) = \rho_0 + \rho_1(\mathbf{r}, t) + \rho_2(\mathbf{r}, t), \quad (7a)$$

$$p(\mathbf{r}, t) = p_0 + p_1(\mathbf{r}, t) + p_2(\mathbf{r}, t), \quad (7b)$$

$$\mathbf{v}(\mathbf{r}, t) = \mathbf{v}_0 + \mathbf{v}_1(\mathbf{r}, t) + \mathbf{v}_2(\mathbf{r}, t), \quad (7c)$$

$$\boldsymbol{\tau}(\mathbf{r}, t) = \boldsymbol{\tau}_0 + \boldsymbol{\tau}_1(\mathbf{r}, t) + \boldsymbol{\tau}_2(\mathbf{r}, t), \quad (7d)$$

where subscript 0, 1 and 2 indicate the zeroth, first and second order of perturbation, respectively. The fluid is considered to be at rest in the unperturbed state, so the values of \mathbf{v}_0 and $\boldsymbol{\tau}_0$ is set to be zero. First order variables are considered time-harmonic with angular frequency $\omega = 2\pi f$; so that we have $\mathbf{v}_1(\mathbf{r}, t) = \mathbf{v}_1(\mathbf{r})e^{-i\omega t}$, $\rho_1(\mathbf{r}, t) = \rho_1(\mathbf{r})e^{-i\omega t}$, $p_1(\mathbf{r}, t) = p_1(\mathbf{r})e^{-i\omega t}$, and $\boldsymbol{\tau}_1(\mathbf{r}, t) = \boldsymbol{\tau}_1(\mathbf{r})e^{-i\omega t}$. In isentropic cases, we have $p_1 = c_0^2 \rho_1$, where c_0 is the speed of sound³⁶.

By substituting Eq. (7) into the Eq. (1), the first-order perturbation of the governing equations are obtained as follow,

$$i\omega \rho_1 = \rho_0 \nabla \cdot \mathbf{v}_1, \quad (8a)$$

$$-i\omega \rho_0 \mathbf{v}_1 = -\nabla p_1 + \nabla \cdot \boldsymbol{\tau}_1. \quad (8b)$$

The first-order perturbation of shear stress, $\boldsymbol{\tau}_1$, of viscous fluid is written as,

$$\boldsymbol{\tau}_1 = \eta[\nabla \mathbf{v}_1 + (\nabla \mathbf{v}_1)^T] + [\eta_b - \frac{2}{3}\eta](\nabla \cdot \mathbf{v}_1)\mathbf{I}, \quad (9)$$

and for a viscoelastic fluid, the equation (9) is replaced by the following equation,

$$\boldsymbol{\tau}_1 = \eta^*[\nabla \mathbf{v}_1 + (\nabla \mathbf{v}_1)^T], \quad (10)$$

where $\eta^* = \eta_0/(1 - iDe)$ denotes the complex viscosity, η_0 is the zero shear rate viscosity, and $De = \lambda\omega$ is called Deborah number. At $\lambda = 0$, the viscoelastic fluid behaves like a viscous fluid²⁷.

Considering all fields' time dependency as $e^{-i\omega t}$, and inserting Eqs. (8a) and (9) into the Eq. (8b), the first-order acoustic wave equation for p_1 is obtained as¹²,

$$\nabla^2 p_1 + \frac{\omega^2}{c_0^2} (1 + i\omega \frac{\eta_b + \frac{1}{3}\eta}{c_0^2 \rho_0}) p_1 = 0. \quad (11)$$

For viscoelastic cases, the first-order acoustic wave equation is expressed by,

$$\nabla^2 p_1 + \frac{\omega^2}{c_0^2} (1 + i\omega \frac{2\eta^*}{c_0^2 \rho_0}) p_1 = 0. \quad (12)$$

Second-order perturbation. The time-averaged second-order perturbation approximation of governing equations for a viscous fluid are expressed by,

$$\nabla \cdot \langle \mathbf{v}_2 \rangle + \kappa_s \langle \mathbf{v}_1 \cdot \nabla p_1 \rangle = 0, \quad (13a)$$

$$\nabla \cdot [\langle \boldsymbol{\tau}_2 \rangle - \langle p_2 \rangle \mathbf{I} - \rho_0 \langle \mathbf{v}_1 \mathbf{v}_1 \rangle] = 0, \quad (13b)$$

where $\kappa_s = \frac{1}{\rho} (\frac{\partial \rho}{\partial p})_s = \frac{1}{\rho_0 c_0^2}$ is the isentropic compressibility in classical fluid mechanics. In the adiabatic limit $p_1 = \rho_0 \kappa_s p_1$. The time-averaged second-order perturbation of shear stress, $\boldsymbol{\tau}_2$, of a viscous fluid is

$$\langle \boldsymbol{\tau}_2 \rangle = \eta \langle \nabla \mathbf{v}_2 + (\nabla \mathbf{v}_2)^T \rangle + [\eta_b - \frac{2}{3}\eta] \langle \nabla \cdot \mathbf{v}_2 \rangle \mathbf{I}. \quad (14)$$

For a viscoelastic fluid, Eq. (14) turns into

$$\begin{aligned} \langle \boldsymbol{\tau}_2 \rangle &= \eta_0 \langle \nabla \mathbf{v}_2 + (\nabla \mathbf{v}_2)^T \rangle \\ &\quad - \lambda \eta^* \langle (\mathbf{v}_1 \cdot \nabla) [\nabla \mathbf{v}_1 + (\nabla \mathbf{v}_1)^T] \rangle \\ &\quad + \lambda \eta^* \langle (\nabla \mathbf{v}_1) \cdot [\nabla \mathbf{v}_1 + (\nabla \mathbf{v}_1)^T] \rangle \\ &\quad + \lambda \eta^* \langle [\nabla \mathbf{v}_1 + (\nabla \mathbf{v}_1)^T] \cdot (\nabla \mathbf{v}_1)^T \rangle . \end{aligned} \quad (15)$$

In the above equations the time average over full oscillation period, T , of each quantity, $Y(t)$, is defined as,

$$\langle Y \rangle = \frac{1}{T} \int_0^T Y(t) dt . \quad (16)$$

The physical, real-valued time average of two harmonically varying fields with the complex representation, is given by

$$f(\mathbf{r}, t) = f(\mathbf{r}) e^{-i\omega t} , \quad (17a)$$

$$g(\mathbf{r}, t) = g(\mathbf{r}) e^{-i\omega t} , \quad (17b)$$

$$\langle fg \rangle = \frac{1}{2} \text{Re}[f^* g] . \quad (17c)$$

where the asterisk denotes complex conjugation and $\text{Re}[\]$ shows the physical real value.

Acoustic radiation force. In this section, the acoustic radiation force applied to microparticles, immersed in viscous and viscoelastic fluids in a standing plane wave, are studied. In our manuscript, the first-order scattering theory is used, because the particles' size is much smaller than the incident acoustic wavelength and they act as weak scattering points. The acoustic radiation force is obtained using the inviscid theory. This is a correct approximation for particles extremely larger than the viscous penetration depth $\delta = \sqrt{2\nu/\omega}$ (ν is the kinematic viscosity)¹². At first, a single particle, and then a pair of particles suspended in viscous and viscoelastic fluids in a standing plane wave (at room temperature) are studied. The incoming wave is described by the velocity field \mathbf{v}_{in} , and the outgoing wave from the particle is described by the velocity field \mathbf{v}_{sc} . Therefore, the first-order velocity field \mathbf{v}_1 is expressed by

$$\mathbf{v}_1 = \mathbf{v}_{in} + \mathbf{v}_{sc} . \quad (18)$$

The acoustic radiation force acting on each particle is obtained by

$$\begin{aligned} \mathbf{F}_{rad} &= - \int_{\partial\Omega} da (\langle p_2 \rangle \mathbf{n} + \rho_0 \langle (\mathbf{n} \cdot \mathbf{v}_1) \mathbf{v}_1 \rangle) \\ &= - \int_{\partial\Omega} da \left(\left[\frac{\kappa_s}{2} \langle p_1^2 \rangle - \frac{\rho_0}{2} \langle v_1^2 \rangle \right] \mathbf{n} + \rho_0 \langle (\mathbf{n} \cdot \mathbf{v}_1) \mathbf{v}_1 \rangle \right) , \end{aligned} \quad (19)$$

where $\partial\Omega$ is the particle's surface, and \mathbf{n} is the unit-vector normal to the surface.

Numerical model and boundary conditions. As shown in Fig. 1, a microchannel with a square cross-section of the size, $b = 500 \mu\text{m}$ in the XY plane is considered. The incident wave is a resonant pressure wave of the form

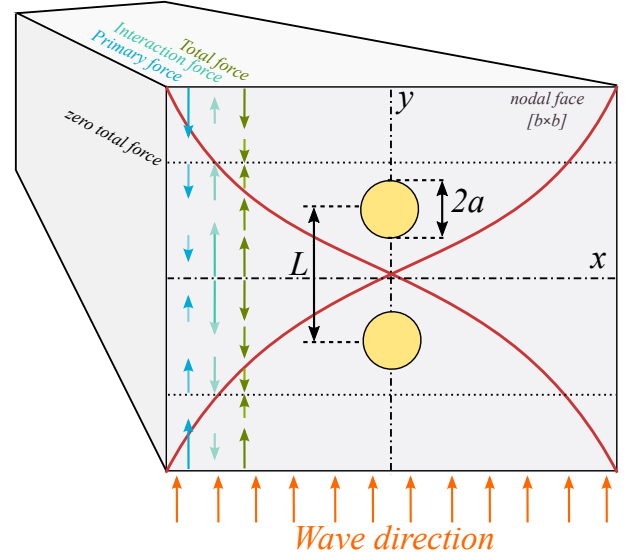


FIG. 1. Configuration of a pair of spheres in a microchannel. L is the center-to-center distance between two particles with a radius of a .

$p = p_{amp} \sin(2\pi y/w)$, in which w and p_{amp} are the wavelength and the amplitude of the wave. In our simulation, the sphere's diameter is considered $8 \mu\text{m}$.

The governing equations are solved for one- and two-particle systems of spheres suspended in viscous and viscoelastic fluids using the finite element method. The weak-form-PDE is used to solve these equations^{37,38}. In the weak-form-PDE method, first, the flow equations are written as source-free flux formulation, $\nabla \cdot \mathbf{J} + F = 0$. Then, they are converted to the weak-form. At the end, the weak-form equations are solved by finite element method.

Considering \mathbf{J} as a vector and F as a scalar (e.g. equations 8a and 13a), the weak form of a source-free flux equation is given by

$$\int_{\Omega} \left[-\nabla \tilde{\psi} \cdot \mathbf{J} + \tilde{\psi} F \right] d\mathbf{r} = 0 , \quad (20)$$

where $\tilde{\psi}$ is a test function. For \mathbf{J} as a tensor and F as a vector (e.g. equations 8b and 13b), the weak form of a source-free flux equation is

$$\int_{\Omega} \left[-\nabla \tilde{\Psi}_m \cdot \mathbf{J} + \tilde{\Psi}_m \cdot \mathbf{F} \right] d\mathbf{r} = 0 , \quad \text{for all } m \quad (21)$$

where $\tilde{\Psi}_m$ is the m -th component of a test vector $\tilde{\Psi}$. In all cases, the zero-flux boundary condition, $\mathbf{J} \cdot \mathbf{n} = 0$, is considered. All boundaries of Fig. 1 including microchannel and particles, except the bottom wall, are considered as hard walls. Therefore, the velocity field for these boundaries is $\mathbf{v} \cdot \mathbf{n} = 0$. For the bottom wall the boundary condition is $p = p_{amp} \sin(2\pi y/w)$.

The maximum mesh size on particles' boundaries is equal to $0.01 \mu\text{m}$, and $2 \mu\text{m}$ in bulk region. The mesh

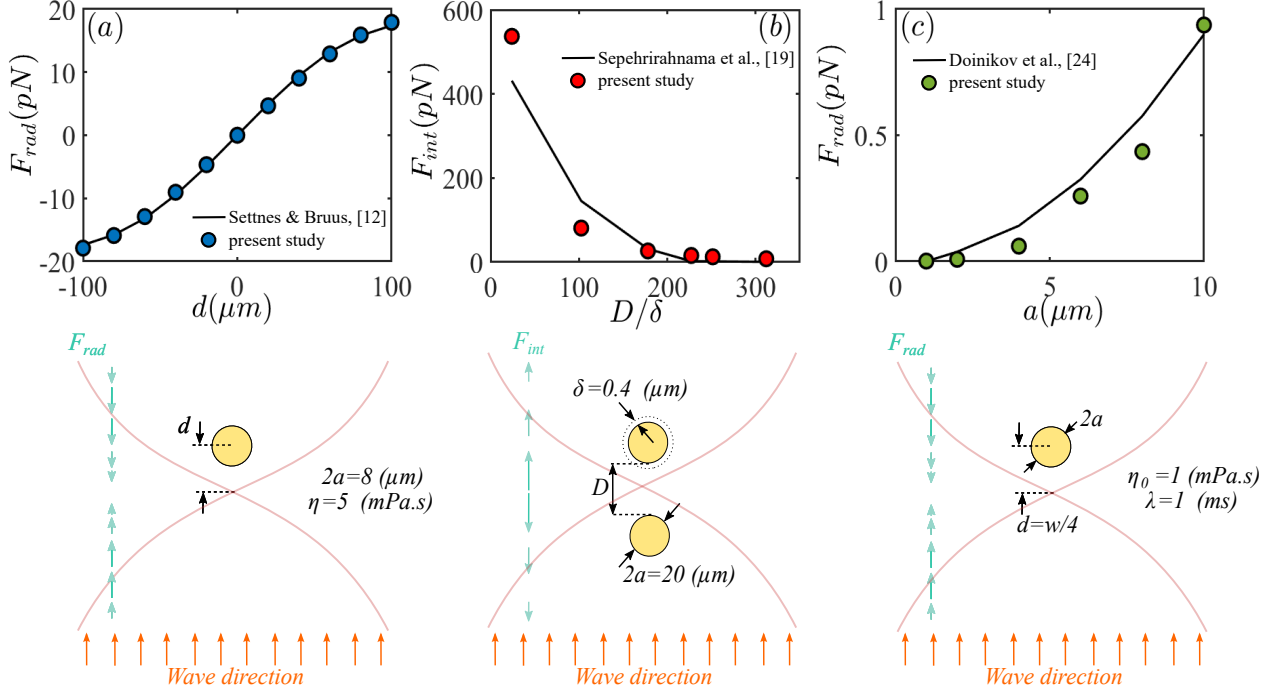


FIG. 2. (a) Acoustic radiation force on a sphere with $a = 4 \mu\text{m}$ in a viscous fluid. (b) Acoustic interaction force between a pair of spheres with $a = 10 \mu\text{m}$ in a viscous fluid. (c) Acoustic radiation force on a polystyrene particle in a viscoelastic fluid.

TABLE I. Physical parameters of fluids and incident acoustic wave at $T = 25^\circ\text{C}$ and $p_0 = 0.1013 \text{ MPa}$. $\eta_0 = 16.9 \text{ mPa}\cdot\text{s}$ and $\lambda = 7.8 \text{ ms}$ are the real experimental data^{12,39}.

Parameter	Symbol	Value	Unit
Wave amplitude	p_{amp}	1	bar
Wave length	w	1000	μm
Actuation frequency	f	1.5	MHz
Mass density	ρ_0	1000	kg/m^3
Speed of sound	c_0	1500	m/s
Bulk viscosity	η_b	2.485×10^{-3}	$\text{Pa}\cdot\text{s}$
Zero shear rate viscosity	η_0	5, 9, 16.9, 25	$\text{Pa}\cdot\text{s}$
Relaxation time	λ	0, 0.6, 4, 7.8, 16	ms

element growth rates on particles' boundaries and in bulk are 1.0003 and 1.1, respectively. The fluid inside the microchannel is supposed to be a quiescent viscous and viscoelastic fluid. The physical parameters of fluids and the incident acoustic wave at temperature $T = 25^\circ\text{C}$ and pressure $p_0 = 0.1013 \text{ MPa}$ are presented in Table I.

By solving the governing equations, the pressure and velocity fields are obtained. Then the acoustic radiation forces are calculated by Eq. (19).

Validation. In order to verify our using method in this contribution, the obtained results for the case of one-particle system surrounded by viscous fluid are compared with those reported by Settnes and Bruus¹². For this purpose, a $4 - \mu\text{m}$ solid sphere ($ka = 0.025 \ll 1$, $k = 2\pi/w$ is the wave number) is considered with its particle-

distance d from the pressure node. The host fluid has a viscosity of $\eta = 5 \text{ mPa}\cdot\text{s}$, density of $\rho_0 = 1000 \text{ kg}/\text{m}^3$, and the speed of sound $c_0 = 1500 \text{ m}/\text{s}$. The frequency of the standing wave is 1.5 MHz and its wavelength is $1000 \mu\text{m}$. The pressure amplitude is 1 bar .

Figure 2(a) shows the acoustic radiation force acting on the sphere for various d . It can be seen that our simulation results are in very good agreement with Settnes and Bruus results, which actually confirms the correctness of our data.

Besides, we have considered a two-particle system including two $10 - \mu\text{m}$ solid spheres with their surface-to-surface distance D in a viscous fluid with $\delta = 0.4 \mu\text{m}$ and calculated the acoustic interaction force between them. Then, we compared our data with those calculated by Sepehrirahnama et al.¹⁹. The other parameters are as in Fig. 2(a). Our obtained results presented in Fig. 2(b) are in agreement with the data by Sepehrirahnama et al..

Moreover, we have also made a comparison between our results and those of Doinikov et al.²⁴ for the case of one-particle system including a polystyrene particle located halfway between the pressure node and the antinode in a viscoelastic fluid with $\eta_0 = 1 \text{ Pa}\cdot\text{s}$ and $\lambda = 1 \text{ ms}$. The parameters of the particle material are the following: the density $\rho_s = 1050 \text{ kg}/\text{m}^3$, Young's modulus $E = 0.32 \times 10^{10} \text{ Pa}$, and Poisson's ratio $\nu = 0.35$. The frequency of the standing plane wave is 1 MHz and the pressure amplitude is 10 kPa . The other parameters are as in Fig. 2(a). In Fig. 2(c), the vertical axis shows the acoustic radiation force acting on the particle. The results are shown for different particle's radius a . The

results are compatible with their.

Results and discussion. In this contribution, extensive numerical calculations are carried out to study the acoustic radiation forces applied to spherical particles in a two-particle system. The particles suspended in viscous and viscoelastic fluids are exposed to an external standing plane wave. The obtained results indicate that the fluid's rheological parameters like viscosity and relaxation time play important roles on the magnitude of acoustic forces experienced by particles. In the following, results and their implications are discussed.

Total and primary forces. For a two-particle microfluidic system, the total radiation force applied to each particle is divided into the primary and secondary (interaction) forces. The primary force applied to each particle is due to the incoming waves on and scattered waves from the target particle. The secondary force is caused by the scattered waves from the other particle on the target one. First, a two-particle microfluidic system filled with a viscous fluid is considered.

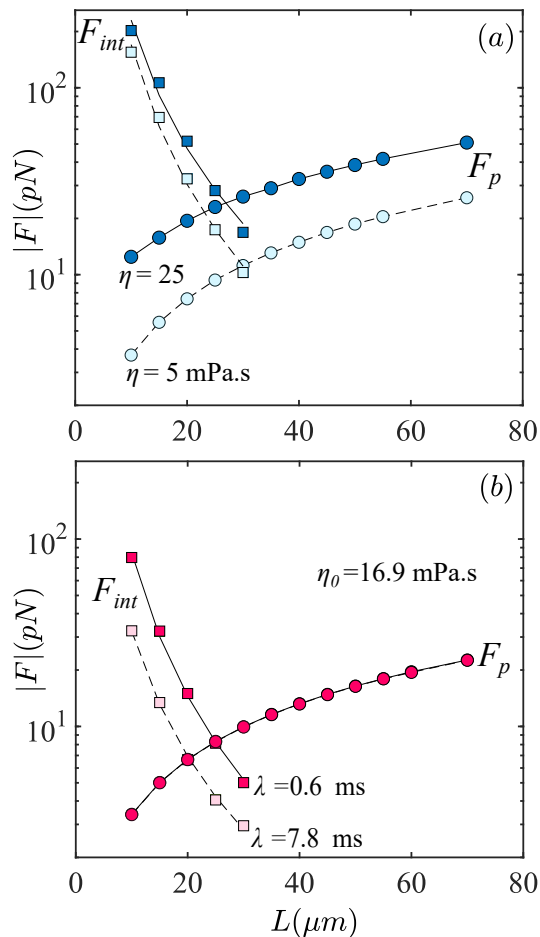


FIG. 3. Primary (\circ) and secondary (\square) forces applied to each particle in a two-particle system for (a) viscous fluids with $\eta = 5$ (---) and 25 mPa.s (—), and (b) viscoelastic fluids with $\eta_0 = 16.9$ mPa.s, $\lambda = 0.6$ (—) and 7.8 ms (---).

In Fig. 3(a), the magnitude of the primary and secondary forces has been plotted in the semi-logarithmic scale for two different values of viscosity. For small L values, the secondary force between two objects is strong. In contrast, the primary force is close to zero. For large distances between the particles, when the spheres are far from the pressure node, the primary force is dominant, while the interaction between the particles becomes noticeably weak. For an intermediate value of L , these two forces neutralize each other. It can be seen that for a definite L value, forces increase with fluid viscosity. Furthermore, it is noticeable that the effect of viscosity on the primary force is more than on the secondary force.

In the next step, the primary and secondary forces for viscoelastic fluids with various λ values are presented in Fig. 3(b). It is clear that the value of the relaxation time play an important role on the magnitude of the interaction force. Besides, the force decreases by λ .

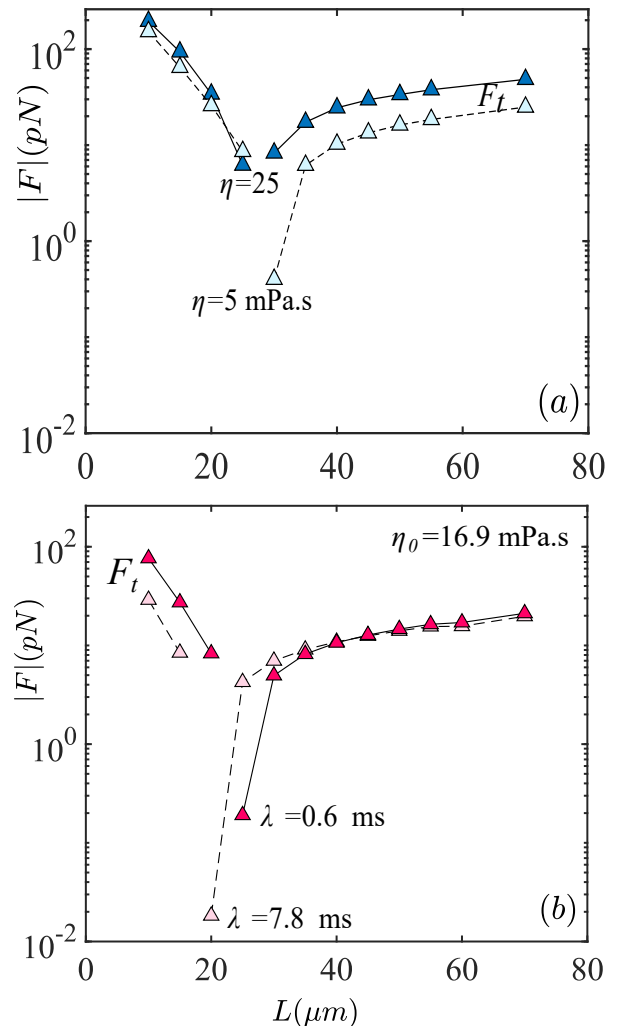


FIG. 4. Total radiation force ($F_t = F_p + F_{int}$) applied to each particle in a two-particle system for (a) viscous fluids with $\eta = 5$ (---) and 25 mPa.s (—), and (b) viscoelastic fluids with $\eta_0 = 16.9$ mPa.s, $\lambda = 0.6$ (—) and 7.8 ms (---).

In Fig. 4(a), the magnitude of the total radiation force

has been shown for different values of η . It can be seen that the total radiation force is large at small distances which is due to the large interaction force between particles in small L values. The total force has a discontinuity in the graph and this is because of the zero value of the force, since it cannot be shown on the semi-logarithmic scale. This is where the primary and secondary forces balance each other. By increasing the inter-particle distance, the interaction force is negligible, so the total and primary forces are almost equal.

The total force for viscoelastic fluids with various λ values are presented in Fig. 4(b). The zero value of total force occurs in smaller L for larger λ values, in compatible with the relation $\eta^* = \eta_0/(1-i\lambda\omega)$ and the results of Fig. 4(a).

The acoustic interaction force between spheres is examined in detail in the following.

Acoustic interaction force. Figure 5 represents the acoustic interaction force between two spheres suspended in a viscous fluid as a function of fluid viscosity η and inter-particle distance L . The data show that the value of F exponentially decreases by L as $\ln F = A(\eta)L + B(\eta)$, compatible with the results shown in Fig. 2(b). The functionality of A and B are presented as insets. According to these data one may write the interaction forces between two spheres as

$$F(L, \eta) = \exp [(0.006 \ln \eta - 0.15)L + (0.14 \ln \eta + 6.09)] . \quad (22)$$

Equation (22) indicates for a definite inter-particle distance, F increases by η .

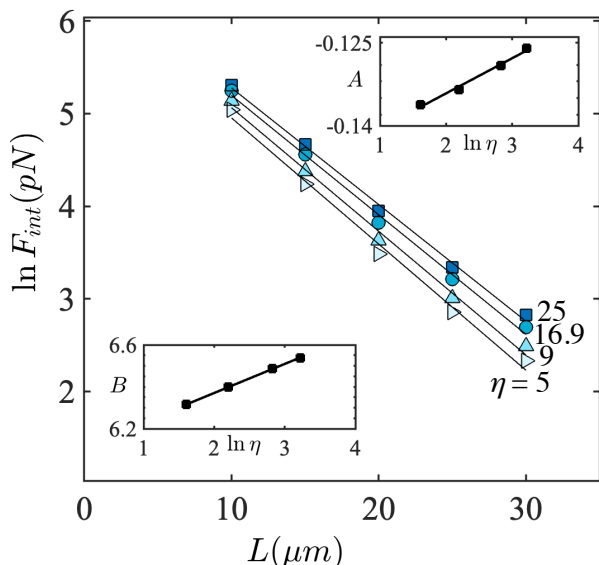


FIG. 5. Acoustic interaction force between two spheres for viscous fluids with $\eta = 5$ (\blacktriangleright), 9 (\blacktriangle), 16.9 (\bullet) and 25 (\blacksquare) *mPa.s*. Insets are the slopes (A) and intercepts (B) of $\ln F(L, \eta)$.

In the next step, we obtain the acoustic interaction force between a pair of spheres suspended in a viscoelastic fluid. The interaction force between two particles as a function of L for various η_0 and λ is plotted in Figs. 6(a)

– 6(d). The results show that for definite λ values, F behaves as a decreasing power-law function of L . Therefore, we can consider the interaction force as $F = m_2 L^{m_1}$. The functionality of m_1 and m_2 versus λ for various η_0 are plotted in Figs. 6(e) and 6(f), respectively. Insets are the slopes of m_1 and m_2 as functions of η_0 . By fitting all these data the interaction force is obtained as,

$$F(L, \eta_0, \lambda) = [(-1986.5 \ln \eta_0 - 2695.5) \ln \lambda + 8733.7 \ln \eta_0 - 927.49] \times L^{(0.76 \lambda \eta_0^{-0.33} - 0.07 \ln \eta_0 - 2.34)} . \quad (23)$$

Equation (23) shows that F increases by fluid's viscosity and decreases by its relaxation time. This mathematical formula shows the behavior of the interaction force between two spherical particles located close to each other immersed in a viscoelastic fluid that no one has obtained until now.

Conclusion. In this letter, it could be viewed as the first simulational modeling of the acoustic interaction force between two spherical particles immersed in a viscoelastic fluid was developed. We have used the first- and second-order perturbation theories for the governing equations to develop the mathematical model based on the Upper-Convected Maxwell equation.

In order to validate the developed mathematical model, firstly we compared it with the literature. We initially verified it for the case of one particle system surrounded by a viscous fluid with the results obtained by Settnes and Bruus¹². Then, for the case of a two-particle system in a viscous fluid, the results were compatible with those calculated by Sepehrirahnama et al.¹⁹. Finally, we made a comparison between our results and those of Doinikov et al.²⁴ for the case of a one-particle system in a viscoelastic fluid. The results were in agreement with those obtained by the literature. Indeed, in the presented model, the particles' radius should be much smaller than the acoustic wavelength and bigger than the viscous penetration depth.

We concluded that the interaction force between the spherical particles is larger for viscous fluids compared to viscoelastic ones at the same zero shear rate viscosity values. This occurred due to the relaxation time effect. In fact, this letter presents the dependence of interaction force on the rheological parameters of the fluid media in which the particles are immersed. In addition, we showed that the interaction force increases by the viscosity and reduces by the relaxation time. A decreasing exponential function of inter-particle distance was obtained, by fitting simulation data, for the interaction force between particles suspended in the viscous fluid. However, a power-law function was obtained in the case of a viscoelastic one. In future work, the effect of drag force as a function of particles' size induced by acoustic streaming, and particle concentration will be considered in a viscoelastic media.

¹L. V. King, On the acoustic radiation pressure on spheres. *Proc. R. Soc. Lond. A* **147**, 212-240 (1934).

²Crum, L. A. Bjerknes forces on bubbles in a stationary sound field. *J. Acoust. Soc. Am* **57**, 1363-1370 (1975).

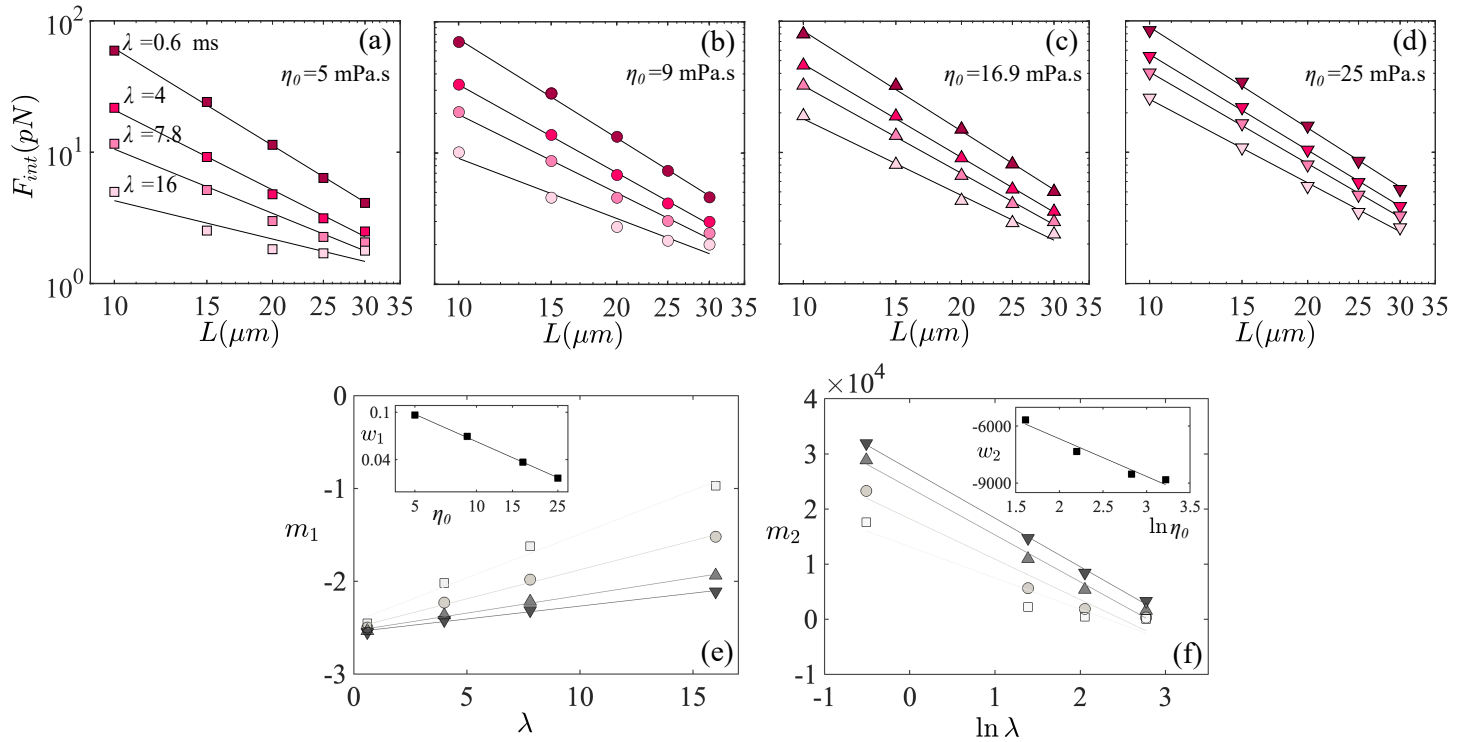


FIG. 6. Acoustic interaction force between a pair of spheres versus L for viscoelastic fluid with viscosities (a) $\eta_0 = 5$, (b) 9, (c) 16.9, and (d) 25 $mPa.s$. The data are for $\lambda = 0.6$ (■), 4 (■), 7.8 (■) and 16 (■) ms . (e) The slopes and (f) intercepts of $F(L, \eta, \lambda)$ for viscosities $\eta = 5$ (■), 9 (●), 16.9 (▲), 25 (▼) $mPa.s$. Insets show slopes of m_1 and m_2 .

- ³Embleton, T. F. W. Mutual interaction between two spheres in a plane sound field. *J. Acoust. Soc. Am* **34**, 1714-1720 (1962).
- ⁴Fox, F. E. Sound pressure on spheres. *J. Acoust. Soc. Am* **12**, 147-149 (1940).
- ⁵Gorkov, L. P. On the forces acting on a small particle in an acoustical field in an ideal fluid. *Sov. Phys. Dokl* **6**, 773-775 (1962).
- ⁶Yosioka, K. & Kawasima, Y. Acoustic radiation pressure on a compressible sphere. *Acustica* **5**, 167-173 (1955).
- ⁷Hasegawa, T., Saka, K., Inoue, N. & Matsuzawa, K. Acoustic radiation force experienced by a solid cylinder in a plane progressive sound field. *J. Acoust. Soc. Am* **83**, 1770-1775 (1988).
- ⁸Mitri, F. G. Acoustic radiation force acting on elastic and viscoelastic spherical shells placed in a plane standing wave field. *Ultrasonics* **43**, 681-691 (2005).
- ⁹Mitri, F. G. Acoustic radiation force acting on absorbing spherical shells. *Wave motion* **43**, 12-19 (2005).
- ¹⁰Doinikov, A. A. Acoustic radiation interparticle forces in a compressible fluid. *J. Fluid Mech.* **444**, 1-21 (2001).
- ¹¹Mitri, F. G. Calculation of the acoustic radiation force on coated spherical shells in progressive and standing plane waves. *Ultrasonics* **44**, 244-258 (2006).
- ¹²Settnes, M. & Bruus, H. Forces acting on a small particle in an acoustical field in a viscous fluid. *Phys. Rev. E* **85**, 016327 (2012).
- ¹³Doinikov, A. A. Bjerknes forces between two bubbles in a viscous fluid. *J. Acoust. Soc. Am* **106**, 3305-3312 (1999).
- ¹⁴Silva, G. T. & Bruus, H. Acoustic interaction forces between small particles in an ideal fluid. *Phys. Rev. E* **90**, 063007 (2014).
- ¹⁵Lopes, J. H., Azarpeyvand, M., Silva, G. T. Acoustic Interaction Forces and Torques Acting on Suspended Spheres in an Ideal Fluid. *IEEE Trans. Ultrason. Ferroelectr. Freq. Control* **63**, 186-197 (2016).
- ¹⁶Zheng, X., Apfel, R. E. Acoustic interaction forces between two fluid spheres in an acoustic field. *J. Acoust. Soc. Am* **97**, 2218-2226 (1995).
- ¹⁷Doinikov, A. A. Viscous effects on the interaction force between two small gas bubbles in a weak acoustic field. *J. Acoust. Soc. Am* **111**, 1602-1609 (2000).
- ¹⁸Sepehrirahnama, S., Lim, K. M., Chau, F. S. Numerical study of interparticle radiation force acting on rigid spheres in a standing wave. *J. Acoust. Soc. Am* **137**, 2614-2622 (2015).
- ¹⁹Sepehrirahnama, S., Chau, F. S., & Lim, K. M. Effects of viscosity and acoustic streaming on the interparticle radiation force between rigid spheres in a standing wave. *Phys. Rev. E* **93**, 023307 (2016).
- ²⁰Pelekasis, N. A., Gaki, A., Doinikov, A. A. & Tsamopoulos, J. A. Secondary Bjerknes forces between two bubbles and the phenomenon of acoustic streamers. *J. Fluid Mech.* **500**, 313347 (2004).
- ²¹Doinikov, A. A., & Zavtrak, S. T. On the mutual interaction of two gas bubbles in a sound field. *Phys. Fluids* **7**, 1923-1930 (1995).
- ²²Doinikov, A. A., & Zavtrak, S. T. Radiation forces between two bubbles in a compressible liquid. *J. Acoust. Soc. Am* **102**, 1424-1431 (1997).
- ²³Silva, G. T. & Bruus, H. Acoustic interaction forces between small particles in an ideal fluid. *Phys. Rev. E* **90**, 063007 (2014).
- ²⁴Doinikov, A. A., Fankhauser, J. and Dual, J. nonlinear dynamics of a solid particle in an acoustically excited viscoelastic fluid. II. Acoustic radiation force. *Phys. Rev. E* **104**, 065108 (2021).
- ²⁵Bahrani, S. A., Périnet, N., Costalonga, M., Royon, L. and Brunet, P. Vortex elongation in outer streaming flows. *Experiments in Fluids* **61**, 1-16 (2020).
- ²⁶Morozov, A. & Spagnolie, S. E. Introduction to Complex Fluids. In: *Complex Fluids in Biological Systems*. Springer, 3-52 (2015).
- ²⁷Hintermuller, M. A., Reichel, E. K., Jakoby, B. Modeling of acoustic streaming in viscoelastic fluids. *IEEE SENSORS*, 1-3 (2017).
- ²⁸Muller, P. B. & Bruus, H. Numerical study of thermoviscous effects in ultrasound-induced acoustic streaming in microchannels. *Phys. Rev. E* **90**, 043016 (2014).

- ²⁹Lei, J., Hill, M. & Glynne-Jones, P. Numerical simulation of 3D boundary-driven acoustic streaming in microfluidic devices. *Lab Chip* **14**, 532–541 (2014).
- ³⁰Hintermüller, M. A., Jakoby, B. & Reichel, E. K. Numerical and experimental analysis of an acoustic micropump utilizing a flexible printed circuit board as an actuator. *Sensor Actuat. A-Phys* **260**, 220–227 (2017).
- ³¹Joseph, D. D. Models Like Maxwell’s and Boltzmann’s. In: Fluid Dynamics of Viscoelastic Liquids. *Springer* **84** 1–34 (1990).
- ³²Oldroyd, J. G. On the Formulation of Rheological Equations of State. *Proc. R. Soc. London, Ser. A* **200**, 523–541 (1950).
- ³³Landau, L. D. & Lifshitz, E. M. Fluid Mechanics, 2nd ed. *Elsevier* **6**, 212–240 (1993).
- ³⁴Lighthill, J. Waves in Fluids. *Cambridge University Press*, (2002).
- ³⁵Pierce, A. D. Acoustics. *J. Acoust. Soc. Am* n**91**, 519-519 (1991).
- ³⁶Bruus, H. Acoustofluidics 2: Perturbation theory and ultrasound resonance modes. *Lab Chip* **12**, 20–28 (2012).
- ³⁷Jannesar, E. A., Hamzhepour, H. Repetitive acoustic streaming patterns in sinusoidal shaped microchannels. *Arch. Acoust* **45**, 35-48 (2020).
- ³⁸Jannesar, E. A., Hamzhepour, H. Acoustic tweezing of microparticles in microchannels with sinusoidal cross sections. *Sci Rep* **11**, 1-14 (2021).
- ³⁹Brust, M., Schaefer, C., Doerr, R., Pan, L., Garcia, M., Arratia, P. E., & Wagner, C. Rheology of Human Blood Plasma: Viscoelastic Versus Newtonian Behavior. *Phys. Rev. Lett* **110**, 078305 (2013).